increase in systolic blood pressure at rest (115.8 ± 2 mm Hg for –/– and 108 ± 1.8 mm Hg for +/+, as measured by the tail cuff method; $P = 0.016$, $n = 8$ for each).

We have shown that $P2X_1$ receptors are involved in the contraction of the vas deferens and that $P2X_1$ receptor deficiency results in a 90% decrease in male fertility through a reduction in sperm in the ejaculate associated with a decrease in neurogenic vas deferens contraction. In mice it appears that the residual α_1-adrenoceptor-mediated neurogenic vas deferens contraction is insufficient for normal ejaculatory function. Selective α_1-adrenoceptor antagonists do not cause azoospermia and infertility in man[17] and contractile studies have indicated the presence of a substantial non-adrenergic component of contraction of prostatic portions of the human vas deferens[18]. This suggests that $P2X_1$-receptor antagonists may provide a target for the development of a non-hormonal male contraceptive pill. In addition, agents that potentiate the actions of ATP at $P2X_1$ receptors may be useful in the treatment of male infertility[19]. □

Methods

Generation of $P2X_1$ receptor-deficient mice

The targeting vector includes 5.8 kilobases (kb) of $P2X_1$-receptor genomic DNA, the *lacZ* gene, the neo^R gene driven by the TK promoter and the HSV-tk gene. Homologous recombination of this vector with the wild-type gene results in deletion of 350 bp of DNA which includes exon 1 and the initiating ATG. The deleted 350 bp are replaced by the *lacZ* gene and the neo^R gene of the targeting vector. The targeting vector was electroporated into E14.1a embryonic stem (ES) cells derived from the 129Ola mouse strain, and colonies were selected with G418 and gancyclovir. Positive colonies were identified by the presence of the 3.7 kb band in *Bam*HI-digested genomic DNA. Four ES colonies containing the targeting event were microinjected into F1 (CBA × C57BL/6) blastocysts and chimaeras were derived. Germline transmission of the targeted allele was obtained from all four ES colonies upon mating to MF-1 animals. The mice analysed here have 129Ola-MF-1 genetic backgrounds.

Immunohistochemistry

Detection of the distribution of the $P2X_1$ receptor using an antibody raised against the C terminus of the receptor was as described[7]. *In vitro* fertilization was as described[20].

Physiological studies

Mice were produced by crossing +/– mice. Littermates were genotyped by PCR, animals were sexually mature (4–6 months old), weight was 37.5 ± 0.8, 39.6 ± 1.3 and 37.3 ± 1.0 g for wild type, +/– and –/–, respectively ($n = 15$–19). Mouse vasa deferentia were mounted in Ringers solution at 36 °C in 15-ml organ baths under an initial load of 1 g, and tension was monitored isometrically. Agonists were applied to the bath at 30-min intervals and removed by washing; this solution was also used for intracellular recordings from the vas deferens using standard methods. Trains of electrical stimuli were delivered through silver chloride electrodes, 20–40 V 0.5 ms pulse width. Vas deferens smooth-muscle cells were enzymatically dissociated and responses to purinergic agonists applied rapidly by a U-tube perfusion system were determined in voltage-clamp recordings as described[21].

Received 22 July; accepted 25 October 1999.

1. Burnstock, G. The past, present and future of purine nucleotides as signalling molecules. *Neuropharmacology* **36,** 1127–1139 (1997).
2. Surprenant, A., Buell, G. & North, R. A. P2X receptors bring new structure to ligand-gated ion channels. *Trends Neurosci.* **18,** 224–229 (1995).
3. Evans, R. J. & Surprenant, A. P2X receptors in autonomic and sensory neurons. *Semin. Neurosci.* **8,** 217–223 (1996).
4. Brading, A. F. & Williams, J. H. Contractile responses of smooth muscle strips from rat and guinea-pig urinary bladder to transmural stimulation: effects of atropine and α,β-methyleneATP. *Br. J. Pharmacol.* **99,** 493–498 (1990).
5. Collo, G. *et al.* Cloning of $P2X_5$ and $P2X_6$ receptors and the distribution and properties of an extended family of ATP-gated ion channels. *J. Neurosci.* **16,** 2495–2507 (1996).
6. Valera, S. *et al.* A new class of ligand-gated ion channel defined by P2X receptor for extracellular ATP. *Nature* **371,** 516–519 (1994).
7. Vulchanova, L. *et al.* Differential distribution of two ATP-gated ion channels (P2X receptors) determined by immunohistochemistry. *Proc. Natl Acad. Sci. USA* **93,** 8063–8067 (1996).
8. Costa, S. L., Boekelheide, K., Vanderhyden, B. C., Seth, R. & McBurney, M. W. Male infertility caused by epididymal dysfunction in transgenic mice expressing a dominant negative mutation of retinoic acid receptors alpha 1. *Biol. Reprod.* **56,** 985–990 (1997).
9. Allcorn, R. J., Cunnane, T. C. & Kirkpatrick, K. Actions of α,β-methylene ATP and 6-hydroxydopamine on sympathetic neurotransmission in the vas deferens of the guinea-pig, rat and mouse: support for co-transmission. *Br. J. Pharmacol.* **89,** 647–659 (1986).
10. von Kugelgen, I., Bultmann, R. & Starke, K. Interaction of adenine nucleotides, UTP and suramin in mouse vas deferens: suramin-sensitive and suramin-insensitive components in the contractile effect of ATP. *Naunyn Schmiedeberg's Arch. Pharmacol.* **342,** 198–205 (1990).
11. Khakh, B. S., Surprenant, A. & Humphrey, P. P. A. A study on P2X purinoceptors mediating the electrophysiological and contractile effects of purine nucleotides in rat vas deferens. *Br. J. Pharmacol.* **115,** 177–185 (1995).
12. Burnstock, G. & Holman, M. E. The transmission of excitation from autonomic nerve to smooth muscle. *J. Physiol.* **155,** 115–133 (1961).
13. Ralevic, V. & Burnstock, G. Receptors for purines and pyrimidines. *Pharmacol. Rev.* **50,** 413–492 (1998).
14. Kenakin, T. in *Pharmacologic Analysis of Drug-Receptor Interaction* Vol. 3, 63–67 (Lippincott-Raven, Philadelphia, 1997).
15. Yang, L. & Clemens, L. G. Influence of male-related stimuli on female postejaculatory refractory period in rats. *Physiol. Behav.* **63,** 675–682 (1998).
16. Anderson, R. A., Oswald, C., Willis, B. R. & Zaneveld, L. J. D. Relationship between semen characteristics and fertility in electroejaculated mice. *J. Reprod. Fertil.* **68,** 1–7 (1983).
17. Hoffman, B. B. & Lefkowitz, R. J. in *The Pharmacological Basis of Therapeutics* (eds Hardman, J. G., Limbird, L. E., Molinoff, P. B., Ruddon, R. W. & Gilman, A. G.) Vol. 9, 199–248 (McGraw-Hill, New York, 1996).
18. Hedlund, H., Andersson, K. & Larsson, B. Effect of drugs interacting with adrenoceptors and muscarinic recetors in the epididymal and prostatic parts of the human isolated vas deferens. *J. Autonom. Pharmacol.* **5,** 261–270 (1985).
19. Jacobson, K. A. *et al.* A pyridoxine cyclic phosphate and its 6-azoaryl derivative selectively potentiate and antagonize activation of P2X1 receptors. *J. Med. Chem.* **41,** 2201–2206 (1998).
20. Hogan, B., Constantini, F. & Lacy, E. *Manipulating the Mouse Embryo: A Laboratory Manual* (Cold Spring Harbour, New York, 1986).
21. Lewis, C., Surprenant, A. & Evans, R. J. 2′,3′-O-(2,4,6-trinitrophenyl) adenosine 5′-triphosphate (TNP-ATP)—a nanomolar affinity antagonist at rat mesenteric artery P2X receptor ion channels. *Br. J. Pharmacol.* 1463–1466 (1998).

Acknowledgements

We thank L. Vulchanova and R. Elde for the $P2X_1$ receptor antibody, B. Grubb and S. Giblett for help with the immunohistochemistry and C. d'Lacey for help with the confocal images. We also thank J. Luckett and S. Monkley for help at the bench and S. R. Nahorski for comments on the manuscript. This work was supported by the Medical Research Council and the Wellcome Trust.

Correspondence and requests for materials should be addressed to R.J.E. (e-mail: RJE6@le.ac.uk).

Turning of nerve growth cones induced by localized increases in intracellular calcium ions

James Q. Zheng

Department of Neuroscience and Cell Biology, University of Medicine and Dentistry of New Jersey, Robert Wood Johnson Medical School, 675 Hoes Lane, Piscataway, New Jersey 08854, USA

Guidance of developing axons involves turning of the motile tip, the growth cone, in response to a variety of extracellular cues[1,2]. Little is known about the intracellular mechanism by which the directional signal is transduced. Ca^{2+} is a key second messenger in growth cone extension[3,4] and has been implicated in growth-cone turning[5,6]. Here I report that a direct, spatially restricted elevation of intracellular Ca^{2+} concentration ($[Ca^{2+}]_i$) on one side of the growth cone by focal laser-induced photolysis (FLIP) of caged Ca^{2+} consistently induced turning of the growth cone to the side with elevated $[Ca^{2+}]_i$ (attraction). Furthermore, when the resting $[Ca^{2+}]_i$ at the growth cone was decreased by the removal of extracellular Ca^{2+}, the same focal elevation of $[Ca^{2+}]_i$ by FLIP induced repulsion. These results provide direct evidence that a localized Ca^{2+} signal in the growth cone can provide the intracellular directional cue for extension and is sufficient to initiate both attraction and repulsion. By integrating local and global Ca^{2+} signals, a growth cone could thus generate different turning responses under different environmental conditions during guidance.

To examine the response of *Xenopus* growth cones to spatially restricted cytosolic Ca^{2+} signals, FLIP of caged Ca^{2+} was used to elevate $[Ca^{2+}]_i$ directly in a spot ~2 μm in diameter. The efficacy and spatial restriction of FLIP was first examined *in vitro* using

4′,5-dimethoxy-2-nitrobenzyl-caged fluorescein-dextran. Simultaneous FLIP and fluorescence imaging showed that a single laser pulse (duration 4 ns, energy ~10 μJ) liberated a significant amount of fluorescence from the caged fluorescein-dextran, indicating effective photoactivation (Fig. 1a). The spatial restriction of FLIP was clearly demonstrated when glycerol was used to slow down the diffusion of dextran molecules[7] (Fig. 1a, upper panel); but without glycerol a much larger radius of fluorescence was observed (Fig. 1a, lower panel). This difference was evident even in the first frame of the sequence when analysed quantitatively (Fig. 1b, c). Next, direct focal elevation of $[Ca^{2+}]_i$ by FLIP was tested using the caged Ca^{2+} compound *o*-nitrophenyl EGTA (NP-EGTA)[8]. Simultaneous FLIP and Ca^{2+} imaging using fluo-3 showed that a single laser pulse induced a localized elevation of $[Ca^{2+}]_i$ in an NP-EGTA-loaded muscle cell, as shown by the spatially restricted increase in fluo-3 fluorescence (Fig. 1e); no change in $[Ca^{2+}]_i$ in the control muscle cell was induced by the laser (Fig. 1d). The localized elevation of $[Ca^{2+}]$ by FLIP was transient and could be detected only in the first frame of the image sequence. Similarly, in growth cones, FLIP of NP-EGTA also induced a spatially restricted elevation of $[Ca^{2+}]_i$ that was observed mostly in the first frame of the image sequence (Fig. 1f). Rapid diffusion as well as cytosolic buffering of the local Ca^{2+} signals[9,10] probably contributes to this transient nature of the focally elevated $[Ca^{2+}]_i$. It should be noted that the imaging results do not accurately represent the focal $[Ca^{2+}]_i$ immediately after FLIP because rapid diffusion alone would probably result in the detection of smaller and more widespread local Ca^{2+} signals. Nevertheless, these results directly demonstrate the spatial restriction of FLIP for direct $[Ca^{2+}]_i$ elevation, which is of critical importance for the experiments below.

To determine whether a local change in $[Ca^{2+}]_i$ at the growth cone is sufficient to signal the direction of extension, $[Ca^{2+}]_i$ on one side of the growth cone was focally elevated by FLIP. Because a relatively long-lasting local Ca^{2+} signal was observed previously during growth cone turning[5], repetitive FLIP of caged Ca^{2+} was performed. To prevent potential damage to the cells from repetitive laser pulses, we reduced the laser energy to ~0.1 μJ per pulse. Repetitive laser irradiation every 3 s produced no effect on the morphology and extension of control growth cones over a 30 min period (Fig. 2a). However, repetitive FLIP of NP-EGTA on one side of the growth cone induced a marked turning response of the growth cone towards the side with $[Ca^{2+}]_i$ elevation within 30 min (Fig. 2b). The attraction involved the preferential protrusion of lamellipodia and filopodia on the FLIP side followed by rapid turning of the growth cone shaft (Fig. 2c; see also Fig. 3a, b). The paths of neurite extension of all the cells loaded with (Fig. 2e) or without (Fig. 2d) NP-EGTA during the 30 min exposure to laser pulses are presented as composite drawings. Of 19 NP-EGTA-loaded growth cones that extended during 30 min of repetitive FLIP, 18 exhibited attractive turning (Fig. 2e), whereas no preferential turning was observed for 14 control growth cones (Fig. 2d). To quantify the turning response, we measured the turning angle and length of neurite extension of each growth cone[5], where positive angles indicate attraction (Fig. 2f, g). Significant attractive turning was observed for growth cones loaded with NP-EGTA, whereas growth cones without NP-EGTA loading were not affected by the repetitive laser irradiation (average turning angle (±s.e.m.): 29.8 ± 4.0 degrees and −5.8 ± 4.8 degrees, respectively; $P < 0.0001$, Kruskal–Wallis test). Both groups of growth cones showed similar lengths of extension over the 30 min period (12.8 ± 0.7 μm and 9.7 ± 1.1 μm, respectively; $P > 0.01$, Kruskal–Wallis test). These results show that direct focal elevation of $[Ca^{2+}]_i$ on one side of the growth cone is sufficient to specifically initiate attractive turning.

To examine the influence of extracellular Ca^{2+} on the turning behaviour of growth cones induced by the direct focal elevation of $[Ca^{2+}]_i$, NP-EGTA loaded cells were placed in a Ca^{2+}-free medium[11] for turning experiments. The removal or marked decrease in extracellular Ca^{2+} concentration in *Xenopus* cultures increased the rate of neurite extension to about three times that in medium containing millimolar Ca^{2+} (refs 5,12,13). Thus, the turning response of the growth cone was examined after only 10 min of repetitive FLIP for a comparable length of extension to that found in Ca^{2+}-containing medium. The same intensity and frequency of laser pulses were found to cause the growth cone in Ca^{2+}-free medium to turn away from the side of FLIP (repulsion). The switching from attraction to repulsion induced by the same repetitive FLIP in different extracellular media is best illustrated in Fig. 3. The particular growth cone shown was induced to turn four times by repetitive FLIP of NP-EGTA: attraction twice in culture medium and repulsion twice in Ca^{2+}-free medium (summarized in Fig. 3e). By alternating the location of the laser beam between the two sides of the growth cone, it was clear that direct focal elevation of $[Ca^{2+}]_i$ consistently induced attractive turning in Ca^{2+}-containing culture medium (Fig. 3a, b) and repulsive turning in Ca^{2+}-free medium (Fig. 3c, d). The attractive turning was preceded by the preferential protrusion of lamellipodia and filopodia on the side of FLIP, followed rapidly by the turning of the growth cone shaft. The repulsive turning, in contrast, was accompanied by a local inhibition of filopodia and lamellipodia on the side of FLIP as well as an increased protrusion of lamellipodia and filopodia on the opposite side. Summary and quantification of the turning response for all the growth cones examined in Ca^{2+}-free medium are shown in Fig. 3f and g, respectively. Of 13 NP-EGTA-loaded growth cones, 12 turned away from the FLIP side, a difference that is statistically significant from growth cones without NP-EGTA loading (turning angles −27.2 ± 9.5 degrees and 4.1 ± 6.6 degrees, respectively; $P < 0.005$, Kruskal–Wallis test). Both groups of growth cones extended similar lengths during the 10 min exposure to laser pulses (13.4 ± 1.4 μm and 14.5 ± 1.8 μm, respectively; $P > 0.1$,

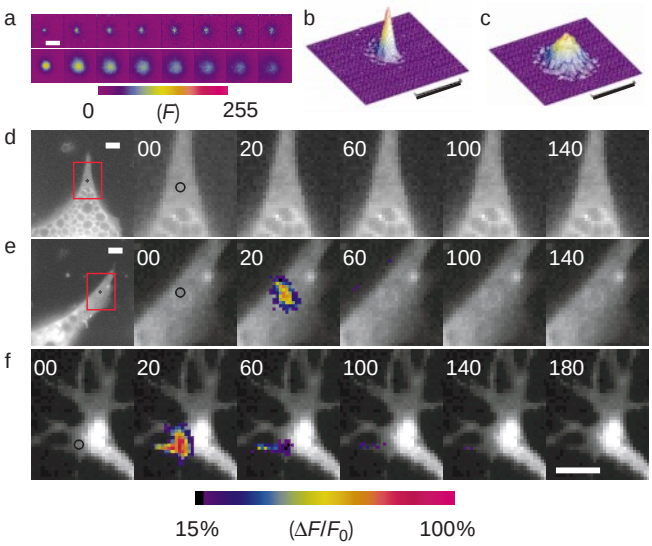

Figure 1 Spatially restricted FLIP of caged molecules. **a**–**c**, Spatiotemporal properties of fluorescence signals produced by FLIP of caged fluorescein-dextran *in vitro*. Two image sequences (**a**) demonstrate different diffusion rates of uncaged fluorescein-dextran in solutions with (upper) and without (lower) glycerol. The interval between each frame is 100 ms and the intensity of the fluorescence (*F*) is pseudo-colour-coded by using the look-up table illustrated in the colour bar shown. Three-dimensional intensity profiles of the first frame of each sequence are shown in **b** (with glycerol) and **c** (without glycerol). **d**, **e**, Localized Ca^{2+} signals produced by single FLIP of NP-EGTA in muscle cells. Image sequences of the Ca^{2+} signal ($\Delta F/F_0$ in pseudo-colour) of a muscle cell without (**d**) and with (**e**) NP-EGTA loading. Boxes indicate the area shown in time sequences, circles illustrate the laser spot, and digits represent milliseconds after a single laser pulse. **f**, Focal increase in $[Ca^{2+}]_i$ in a *Xenopus* growth cone induced by single FLIP of NP-EGTA. Scale bars, 10 μm.

Kruskal–Wallis test), indicating the specificity of focal elevation of $[Ca^{2+}]_i$ on the direction of growth cone extension.

The switching from attraction to repulsion does not seem to involve extracellular actions of Ca^{2+} in the medium directly. When extracellular Ca^{2+} was not completely removed but was decreased to 1.3 μM using a Ca^{2+} buffer[14], repulsion was still induced by repetitive FLIP of NP-EGTA (9 of 10 growth cones; turning angle -21.1 ± 6.1 degrees; average length 13.5 ± 1.9 μm). The removal

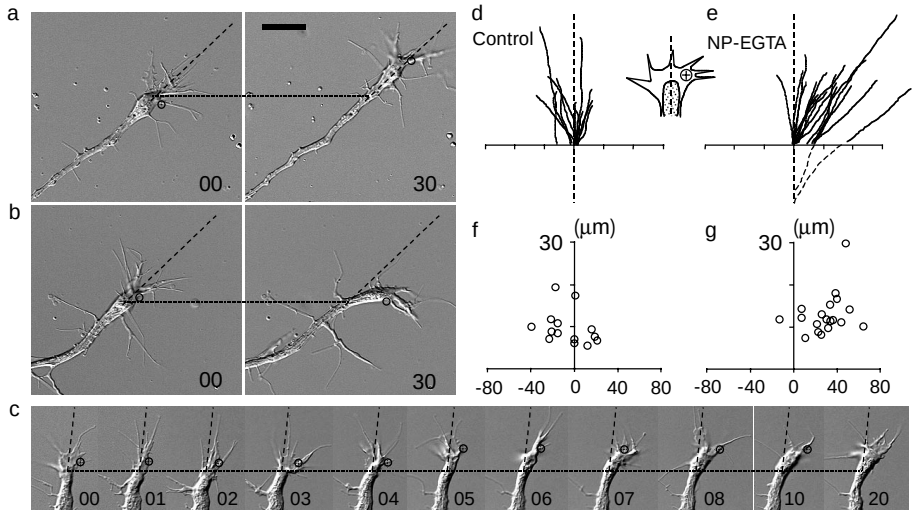

Figure 2 Attractive turning of *Xenopus* growth cones induced by repetitive FLIP of NP-EGTA. **a**, A control growth cone (no NP-EGTA loading) at the beginning and end of 30-min repetitive laser irradiation; circles indicate the laser spot. Dashed lines represent the original direction of extension, and dotted lines represent the corresponding positions along the neurite. **b**, An NP-EGTA-loaded growth cone at the onset and the end of 30-min repetitive FLIP. **c**, A time-lapse sequence of the attractive turning of a growth cone induced by repetitive FLIP of NP-EGTA. Numbers represent minutes after the onset of repetitive FLIP. Scale bars in **a**–**c**, 20 μm. **d**, **e**, Composite drawings of the path of growth cones without (**d**) and with (**e**) NP-EGTA loading during a 30-min exposure to FLIP. Each growth cone was reorientated so that the side of laser irradiation was on the right (illustrated by the diagram in the middle). The origin represents the position of the centre of the growth cone palm at the beginning of the 30-min exposure to the laser. The original direction of growth cone extension was aligned with the vertical axis. Each line depicts the trajectory of the neurite at the end of the 30-min experiment. Tick marks along the horizontal axis represent 5 μm. Note that some growth cones changed their origins, which are represented by the dashed lines. **f**, **g**, Scatter plots of turning angles plotted against length of neurite extension of all the control (**f**) and NP-EGTA-loaded (**g**) growth cones examined.

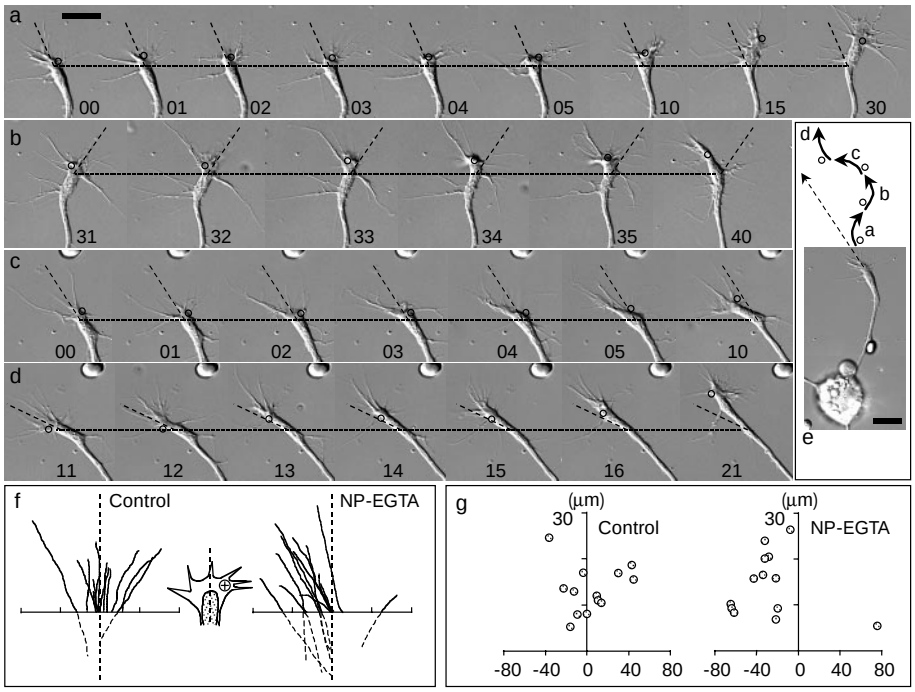

Figure 3 Attractive and repulsive turning of a *Xenopus* growth cone induced by direct focal increase in $[Ca^{2+}]_i$ in different extracellular solutions. **a**, A time-lapse image sequence showing the attractive turning of an NP-EGTA-loaded growth cone induced by repetitive FLIP within 30 min; circles indicate the location of the laser beam. **b**, Attraction was induced for the second time for the same growth cone after repositioning of the laser beam to the other side of the growth cone. **c**, A time-lapse image sequence of the same growth cone, showing repulsive turning when placed in a Ca^{2+}-free medium and exposed to the laser irradiation of same intensity and frequency. **d**, Repulsion was induced for the second time for the same growth cone when the laser was relocated to the opposite side. Numbers in **a**–**d** represent minutes after the onset of FLIP. **e**, Schematic summary of the turning responses of the growth cone (twice attractive and twice repulsive); circles indicate the side of the growth cone on which the laser was applied. Scale bars in **a**–**e**, 20 μm. **f**, Composite drawings of the response of all the growth cones examined in Ca^{2+}-free medium. Tick marks along the horizontal axis represent 5 μm. **g**, Scatter plots of turning angles against length of extension for all the growth cones examined in Ca^{2+}-free medium.

or a significant decrease in extracellular Ca^{2+} concentration is known to affect the resting level of $[Ca^{2+}]_i$ in *Xenopus* neurons[5]. Fura-2 ratiometric imaging showed that replacing Ca^{2+}-containing culture medium with Ca^{2+}-free solution or low-Ca^{2+} buffer immediately decreased the resting $[Ca^{2+}]_i$ at the growth cone from 130.3 ± 17.5 nM to 58.5 ± 5.4 nM or 72 ± 5.0 nM, respectively (means $\pm$ s.e.m.; Fig. 4a–c). To determine whether different resting levels of $[Ca^{2+}]_i$ affect the amount of Ca^{2+} released by FLIP, simultaneous FLIP and fluo-3 imaging were performed. For the reliable detection of small local changes in $[Ca^{2+}]_i$ induced by FLIP of NP-EGTA, the laser energy was increased to 10 μJ. For seven growth cones examined in culture medium, and subsequently in Ca^{2+}-free medium, similar relative changes in fluo-3 fluorescence ($\Delta F/F_0$, calibrated against the corresponding baseline) at the laser spot were observed upon FLIP (Fig. 4d). This result was confirmed by the average of many growth cones examined independently (Fig. 4e; $P > 0.1$, Student's *t*-test). For both culture medium and Ca^{2+}-free medium, a single laser pulse induced a $\Delta F/F_0$ of ~60% at the FLIP spot in the first frame of the image sequence. Assuming that fluo-3 fluorescence corresponds linearly to $[Ca^{2+}]_i$ and by using the resting levels of $[Ca^{2+}]_i$ measured from fura-2 imaging, the peak levels of $[Ca^{2+}]_i$ at the FLIP site are estimated to be ~78 nM and ~35 nM for growth cones in culture medium and in Ca^{2+}-free medium, respectively. It should be emphasized that the Ca^{2+} imaging was performed with laser pulses of ~100 times the intensity used for turning experiments. However, according to the theoretical analysis of point source diffusion[15], the concentration of cytosolic Ca^{2+} at the centre of FLIP at the end of the 20-ms charge-coupled-device (CCD) exposure would have decreased to ~1% of that at 1 ms after photolysis during CCD exposure (14 ms for diffusion).

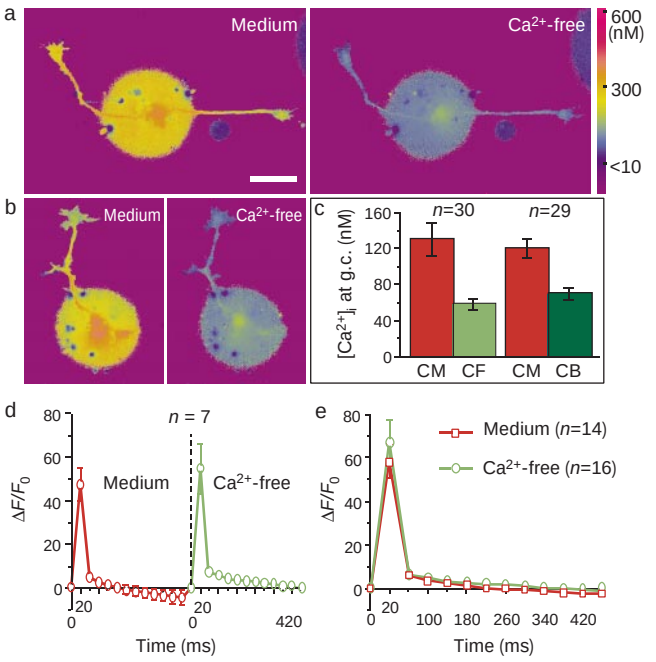

Figure 4 Fluorescence imaging of focal increase in $[Ca^{2+}]_i$ induced by FLIP of NP-EGTA. **a**, **b**, Fura-2 ratio imaging of the resting $[Ca^{2+}]_i$ in a bipolar neuron (**a**) and a monopolar neuron (**b**) in culture medium and Ca^{2+}-free medium. The distribution of $[Ca^{2+}]_i$ is shown in pseudo-colour with the corresponding Ca^{2+} concentration (nM) depicted by the colour bar. **c**, Averages of the resting $[Ca^{2+}]_i$ at the growth cone from populations of neurons in culture medium (CM) and Ca^{2+}-free medium (CF) or in a Ca^{2+}-buffer containing 1.3 μM free Ca^{2+} (CB). **d**, Fluo-3 imaging of the focal increase in $[Ca^{2+}]_i$ at the growth cone induced by FLIP of caged Ca^{2+} in culture medium and Ca^{2+}-free medium. No significant difference was observed in the amplitude of focal $[Ca^{2+}]_i$ increased by FLIP of NP-EGTA for each growth cone examined in these two media. This is confirmed by the average of many growth cones examined (**e**).

Cytosolic buffering of local Ca^{2+} could further decrease the amplitude of the local Ca^{2+} signals that can be detected by the imaging. Taking these two factors into account, the estimate of the actual peak amplitude of the focal $[Ca^{2+}]_i$ elevated by each laser pulse during growth cone turning would be on the same order as that obtained with our imaging measurement, that is, ~78 nM and ~35 nM for growth cones in culture medium and Ca^{2+}-free medium, respectively. Therefore, the removal of extracellular Ca^{2+} decreases the resting $[Ca^{2+}]_i$ as well as the absolute level of focal $[Ca^{2+}]_i$ elevation induced by FLIP of caged Ca^{2+} with the same laser intensity.

To determine whether the resting $[Ca^{2+}]_i$ or the absolute level of focal elevation of $[Ca^{2+}]_i$ contributes to the repulsion, growth cones in Ca^{2+}-free medium were induced to turn by FLIP of NP-EGTA with an increased laser intensity that led to a similar level of focal $[Ca^{2+}]_i$ as that found in culture medium (~70 nM). Of twelve growth cones examined, eight showed marked repulsion, whereas two of the other four growth cones showed no turning and two exhibited attraction (turning angle -15.1 ± 7.5 degrees; average length 17.6 ± 2.4 μm). This result indicates that resting levels of $[Ca^{2+}]_i$ at the growth cone are important in modulating the turning responses. The opposite turning responses might be a reflection of the differential activation of signalling molecules with different thresholds for $[Ca^{2+}]_i$: repulsion results from the activation of intracellular molecules with a low threshold for $[Ca^{2+}]_i$ ($\sim 58 + 35 = 93$ nM), whereas attraction results from the activation of molecules with a high threshold for $[Ca^{2+}]_i$ ($\sim 130 + 78 = 208$ nM). Under normal $[Ca^{2+}]_i$ conditions, signalling molecules of the repulsive mechanism might be saturated or desensitized, allowing only attraction after the focal elevation of $[Ca^{2+}]_i$. Lowering resting $[Ca^{2+}]_i$ allows the low-threshold molecules to be activated by the local Ca^{2+} signals that reach the threshold for repulsion but remain below the threshold for attraction. The ability to finely manipulate the absolute levels of focal $[Ca^{2+}]_i$ elevation in the growth cone by using FLIP will permit further experiments to test this hypothesis.

I have shown that direct focal elevation of $[Ca^{2+}]_i$ on one side of the growth cone is sufficient to initiate both attractive and repulsive turning of the growth cone. Ca^{2+} is a key second messenger that regulates growth cone behaviour[3,4,16–18]. The guidance of growth cones by many diffusible cues such as netrin-1 has been shown to involve Ca^{2+} (refs 13, 14, 19). However, the precise role of Ca^{2+} signals in directional sensing and steering of the growth cone is unclear. Results from this study provide the first direct evidence that a localized increase in $[Ca^{2+}]_i$ at the growth cone can provide the directional signal for growth cone extension and is sufficient to steer the growth cones accordingly. Furthermore, the finding that both local and global (resting) cytosolic Ca^{2+} signals contribute to determining the direction of growth cone turning demonstrates an important feature of intracellular signalling in growth cones for processing and integrating various cellular signals. During neural development *in vivo*, the resting $[Ca^{2+}]_i$ of developing neurons is likely to be influenced and modulated by environmental factors such as adhesion molecules[20]. Furthermore, raising the cAMP concentration in the growth cone has been shown to decrease high $[Ca^{2+}]_i$ (ref. 21). Thus, depending on its surroundings, an axon can respond with either attractive or repulsive turning to the same guidance molecules that act through the Ca^{2+} pathway. With recent findings that the turning direction of growth cones in netrin-1 gradients can be regulated by the cyclic AMP pathway (probably downstream of Ca^{2+})[14] as well as by different cytoplasmic components of the appropriate receptors[22,23], these results indicate the existence of multiple levels of intracellular regulation of directed growth cone extension. Such diversity of regulation along the signal transduction pathway, if it occurred *in vivo*, could provide the potential for the specific and accurate wiring of millions of axons through a limited number of cues available during development. □

Methods

Optical set up

The laser beam (wavelength 337 nm) from a pulsed nitrogen laser (model no. VSL-337N, Laser Science) was introduced into a Nikon TE300 inverted microscope with a laser-to-microscope adapter (Laser Science) mounted on a modified fluorescence epi-illuminator. A dichroic mirror (DM400, Nikon) in the epi-illuminator reflected the laser beam into the microscope while allowing simultaneous fluorescence imaging by using excitation light with wavelengths >400 nm (thus excluding fura-2 imaging). The laser beam was focused into a spot of ~2 μm in diameter with a 40×/1.3 oil-immersion objective (Plan-Fluor., Nikon). A frame-transfer cooled CCD camera (PXL37, Photometrics) was used with the AIW software from Axon Instruments for image acquisition. Each image was acquired by a 20 ms exposure with CCD binning and gain set at 4 and 8, respectively. A sample rate of 25 Hz for a small region of 50 × 50 $(pixel)^2$ was normally achieved. The FLIP and imaging were synchronized by a trigger signal from the computer to fire the laser 5 ms after the onset of the first CCD exposure of the image sequence.

Growth cone turning

Xenopus neurons from 6-h cultures[24,25] were incubated with 6 μM acetoxymethyl (AM) ester derivative of NP-EGTA (Molecular Probes) for 30 min, followed by three washes. Growth cones frequently exhibited a blunt morphology with little motility immediately after loading, so they were left to recover in culture medium for 3 h. This 3-h incubation also allowed further de-esterification of NP-EGTA AM and Ca^{2+} binding by NP-EGTA. Turning experiments were performed in an open microscopy chamber[26]. Each growth cone was positioned such that the laser spot would be located on one side and be kept at the same location throughout the entire experiment. Images of the growth cone at various times after the onset of repetitive FLIP were processed digitally and acquired[25], and quantitative measurement and analysis of the turning response were then performed on these digital images[5,11].

Ca^{2+} imaging

Cells were loaded with 8 μM fluo-3 AM (Molecular Probes) 2 h after the end of NP-EGTA loading for 30 min followed by a 30 min incubation in culture medium. The Ca^{2+} signals were measured by using the change in fluorescence relative to the baseline before the irradiation ($\Delta F/F_0$). All the fluo-3 fluorescence was corrected for background by using the fluorescence from the same cell lysed at the end of the experiment with digitonin[27]. Focal increase in $[Ca^{2+}]_i$ was measured at the FLIP site with a 2-μm diameter zone. For visual presentation of the Ca^{2+} signals, the resulting $\Delta F/F_0$ was given a threshold of 15%, pseudo-coloured and overlaid on a grey-scale image of the cell before the laser irradiation. Fura-2 measurements of the resting $[Ca^{2+}]_i$ was performed with previous methods[5,28]. The cells were typically imaged first in culture medium and then in Ca^{2+}-free medium.

Received 14 September; accepted 20 October 1999.

1. Bray, D. & Hollenbeck, P. J. Growth cone motility and guidance. *Annu. Rev. Cell Biol.* **4,** 43–61 (1988).
2. Tessier-Lavigne, M. & Goodman, C. S. The molecular biology of axon guidance. *Science* **274,** 1123–1133 (1996).
3. Kater, S. B. & Mills, L. R. Regulation of growth cone behavior by calcium. *J. Neurosci.* **11,** 891–899 (1991).
4. Gu, X. & Spitzer, N. C. Distinct aspects of neuronal differentiation encoded by frequency of spontaneous Ca^{2+} transients. *Nature* **375,** 784–787 (1995).
5. Zheng, J. Q., Felder, M., Connor, J. A. & Poo, M. M. Turning of nerve growth cones induced by neurotransmitters. *Nature* **368,** 140–144 (1994).
6. Zheng, J. Q., Poo, M. M. & Connor, J. A. Calcium and chemotropic turning of nerve growth cones. *Perspect. Dev. Neurobiol.* **4,** 205–213 (1996).
7. Ishihara, A., Gee, K., Schwartz, S., Jacobson, K. & Lee, J. Photoactivation of caged compounds in single living cells: an application to the study of cell locomotion. *Biotechniques* **23,** 268–274 (1997).
8. Ellis-Davies, G. C. & Kaplan, J. H. Nitrophenyl-EGTA, a photolabile chelator that selectively binds Ca^{2+} with high affinity and releases it rapidly upon photolysis. *Proc. Natl Acad. Sci. USA* **91,** 187–191 (1994).
9. Connor, J. A. & Ahmed, Z. Diffusion of ions and indicator dyes in neural cytoplasm. *Cell. Mol. Neurobiol.* **4,** 53–66 (1984).
10. Ahmed, Z. & Connor, J. A. Calcium regulation by and buffer capacity of molluscan neurons during calcium transients. *Cell. Calcium* **9,** 57–69 (1988).
11. Zheng, J. Q., Wan, J. J. & Poo, M. M. Essential role of filopodia in chemotropic turning of nerve growth cone induced by a glutamate gradient. *J. Neurosci.* **16,** 1140–1149 (1996).
12. Bixby, J. L. & Spitzer, N. C. Early differentiation of vertebrate spinal neurons in the absence of voltage-dependent Ca^{2+} and Na^+ influx. *Dev. Biol.* **106,** 89–96 (1984).
13. Song, H. J., Ming, G. L. & Poo, M. M. cAMP-induced switching in turning direction of nerve growth cones. *Nature* **388,** 275–279 (1997).
14. Ming, G. L. *et al.* cAMP-dependent growth cone guidance by netrin-1. *Neuron* **19,** 1225–1235 (1997).
15. Lohof, A. M., Quillan, M., Dan, Y. & Poo, M. M. Asymmetric modulation of cytosolic cAMP activity induces growth cone turning. *J. Neurosci.* **12,** 1253–1261 (1992).
16. Kater, S. B. & Rehder, V. The sensory-motor role of growth cone filopodia. *Curr. Opin. Neurobiol.* **5,** 68–74 (1995).
17. Gundersen, R. W. & Barrett, J. N. Characterization of the turning response of dorsal root neurites toward nerve growth factor. *J. Cell Biol.* **87,** 546–554 (1980).
18. Gomez, T. M. & Spitzer, N. C. *In vivo* regulation of axon extension and pathfinding by growth-cone calcium transients. *Nature* **397,** 350–355 (1998).
19. Song, H. *et al.* Conversion of neuronal growth cone responses from repulsion to attraction by cyclic nucleotides. *Science* **281,** 1515–1518 (1998).
20. Snow, D. M., Atkinson, P. B., Hassinger, T. D., Letourneau, P. C. & Kater, S. B. Chondroitin sulfate proteoglycan elevates cytoplasmic calcium in DRG neurons. *Dev. Biol.* **166,** 87–100 (1994).
21. Lankford, K. L. & Letourneau, P. C. Roles of actin filaments and three second-messenger systems in short-term regulation of chick dorsal root ganglion neurite outgrowth. *Cell Motil. Cytoskel.* **20,** 7–29 (1991).
22. Hong, K. *et al.* A ligand-gated association between cytoplasmic domains of UNC5 and DCC family receptors converts netrin-induced growth cone attraction to repulsion. *Neuron* **97,** 427–441 (1999).
23. Bashaw, G. J. & Goodman, C. S. Chimeric axon guidance receptors: the cytoplasmic domains of slit and netrin recetors specify attraction versus repulsion. *Neuron* **97,** 917–926 (1999).
24. Tabti, N. & Poo, M. M. in *Culturing Nerve Cells* (ed. Banker, G. & Goslin, K.) 137–154 (MIT, Cambridge, Massachusetts, 1990).
25. Wang, Q. & Zheng, J. Q. Cyclic AMP-mediated regulation of neurotrophin-induced collapse of nerve growth cones. *J. Neurosci.* **18,** 4973–4984 (1998).
26. Ming, G. L., Lohof, A. M. & Zheng, J. Q. Acute morphogenic and chemotropic effects of neurotrophins on cultured embryonic *Xenopus* spinal neurons. *J. Neurosci.* **17,** 7860–7871 (1997).
27. Kao, J. P., Harootunian, A. T. & Tsien, R. Y. Photochemically generated cytosolic calcium pulses and their detection by fluo-3. *J. Biol. Chem.* **264,** 8179–8184 (1989).
28. Tsien, R. Y. Fluorescence measurement and photochemical manipulation of cytosolic free calcium. *Trends Neurosci.* **11,** 419–424 (1988).

Acknowledgements

I thank R. Maki Fitzsimonds (Yale University, New Haven, Connecticut, USA) and J. Alder (University of Medicine and Dentistry of New Jersey, Robert Wood Johnson Medical School, Piscataway, New Jersey, USA) for their critical review and comments on the manuscript, and J. Gibney for technical support. The initial part of this study was performed at the Marine Biological Laboratory (Woods Hole, Massachusetts, USA) with the support of a Nikon summer fellowship. This work was supported by a grant from the National Institutes of Health.

Correspondence and requests for materials should be addressed to J.Q.Z. (e-mail: zhengiq@umdnj.edu).

Calcium signalling in the guidance of nerve growth by netrin-1

Kyonsoo Hong*†, Makoto Nishiyama*†, John Henley*, Marc Tessier-Lavigne‡ & Mu-ming Poo*

** Department of Biology, University of California at San Diego, La Jolla, California 92093-0357, USA*
‡ Howard Hughes Medical Institute, Department of Anatomy and Department of Biochemistry and Biophysics, University of California at San Francisco, San Francisco, California 94143-0452, USA
† These authors contributed equally to this work

Pathfinding by growing axons in the developing nervous system is guided by diffusible or bound factors that attract or repel the axonal growth cone[1,2]. The cytoplasmic signalling mechanisms that trigger the responses of the growth cone to guidance factors are mostly unknown[3]. Previous studies have shown that the level and temporal patterns of cytoplasmic Ca^{2+} can regulate the rate of growth-cone extension *in vitro*[4–8] and *in vivo*[9]. Here we report that Ca^{2+} also mediates the turning behaviour of the growth cones of cultured *Xenopus* neurons that are induced by an extracellular gradient of netrin-1, an established diffusible guidance factor *in vivo*[1,10]. The netrin-1-induced turning response depends on Ca^{2+} influx through plasma membrane Ca^{2+} channels, as well as Ca^{2+}-induced Ca^{2+} release from cytoplasmic stores[11]. Reduction of Ca^{2+} signals by blocking either of these two Ca^{2+} sources converted the netrin-1-induced response from attraction to repulsion. Activation of Ca^{2+}-induced Ca^{2+} release from internal stores with a gradient of ryanodine in the absence of netrin-1 was sufficient to trigger either attractive or repulsive responses, depending on the ryanodine concentration used. These results support the model that cytoplasmic Ca^{2+} signals mediate growth-cone guidance by netrin-1, and different patterns of Ca^{2+} elevation trigger attractive and repulsive turning responses.

We created a microscopic gradient of netrin-1 in cell cultures by repetitive pulsatile application of netrin-1 from a micropipette[12].